

Consistent relativistic mean-field models: critical parameter values

M. Dutra^{*,1}, O. Lourenço^{*,2} and D. P. Menezes³

¹*Departamento de Ciências da Natureza - IHS, Universidade Federal Fluminense, 28895-532 Rio das Ostras, RJ, Brazil*

²*Universidade Federal do Rio de Janeiro, 27930-560, Macaé, RJ, Brazil*

³*Depto de Física - CFM - Universidade Federal de Santa Catarina, Florianópolis - SC - CP. 476 - CEP 88.040 - 900 - Brazil*

(Dated: November 9, 2018)

We revisit the study published in [1], related to the behavior of 34 relativistic mean-field models, previously selected because they satisfy bulk nuclear matter properties, here used to compute the critical parameters of the symmetric nuclear matter. We evaluate their critical temperature, pressure, and density and compare with some values encountered in the literature. We also show that these parameters are correlated with the incompressibility calculated at the zero temperature regime.

I. INTRODUCTION

Nuclear matter is an idealized medium, and all its properties, are derived from experiments indirectly in a model-dependent way. However, the understanding of its properties is of fundamental importance as a guide towards more specific subjects, such as nuclear and hadron spectroscopy, heavy-ion collisions, nuclear multifragmentation, caloric curves, and others. It is well known that theoretical hadronic models predict phase transitions at moderate temperatures. All these models share the prediction that a liquid-gas phase transition occurs for symmetric and asymmetric nuclear matter at finite temperature and density. Qualitatively, the isotherms of these hadronic mean-field models typically show a van der Waals-like behavior, where liquid and gaseous phases can coexist [2].

It is important to note that the critical temperature is defined in such a way that it always takes place in symmetric matter. In Ref.[3] the authors have shown that the instability region decreases with the increase of the temperature up to a certain value, which is related to a critical pressure and critical density. The values of these critical parameters are model dependent and there are many nonrelativistic and relativistic models in the literature, which can be used to calculate them. In this work we use the Relativistic Mean-Field (RMF) Approximation.

II. CHOICE OF MODELS

Our study is based on the study presented in Ref. [4] where 263 RMF models were analyzed. These parametrizations had their volumetric and thermodynamical quantities compared with theoretical and experimental data available in the literature. These data were

divided into three groups: symmetric nuclear matter (SNM), pure neutron matter (PNM) and a third group named MIX (the mixture of PNM + SNM). This last one encompasses the symmetry energy and its slope at the saturation density as well as reduction of the symmetry energy at half of the saturation density. In Table I we present a summary of these constraints. For more details see Ref. [4].

The analysis has shown that only 35 parametrizations were approved. They are named consistent relativistic mean field (CRMf) parametrizations. We consider in the present study only 34 of them because the point-coupling parametrization does not generate a mass-radius curve, according to Ref. [5], so, it was excluded. The remaining of them are part of two groups out of the seven presented in Ref. [4]. We have shown them in Subsection II A and II B of that reference”.

A. Nonlinear RMF models

The group of the nonlinear RMF parametrizations with σ and ω terms and cross terms involving these fields encompasses thirty parametrizations. The Lagrangian density that describes this model is:

$$\begin{aligned} \mathcal{L}_{\text{NL}} = & \bar{\psi}(i\gamma^\mu\partial_\mu - M)\psi + g_\sigma\sigma\bar{\psi}\psi - g_\omega\bar{\psi}\gamma^\mu\omega_\mu\psi \\ & - \frac{g_\rho}{2}\bar{\psi}\gamma^\mu\vec{\rho}_\mu\vec{\tau}\psi + \frac{1}{2}(\partial^\mu\sigma\partial_\mu\sigma - m_\sigma^2\sigma^2) - \frac{A}{3}\sigma^3 \\ & - \frac{B}{4}\sigma^4 - \frac{1}{4}F^{\mu\nu}F_{\mu\nu} + \frac{1}{2}m_\omega^2\omega_\mu\omega^\mu + \frac{C}{4}(g_\omega^2\omega_\mu\omega^\mu)^2 \\ & - \frac{1}{4}\vec{B}^{\mu\nu}\vec{B}_{\mu\nu} + \frac{1}{2}m_\rho^2\vec{\rho}_\mu\vec{\rho}^\mu + \frac{1}{2}\alpha'_3g_\omega^2g_\rho^2\omega_\mu\omega^\mu\vec{\rho}_\mu\vec{\rho}^\mu \\ & + g_\sigma g_\omega^2\sigma\omega_\mu\omega^\mu \left(\alpha_1 + \frac{1}{2}\alpha'_1g_\sigma\sigma \right) \\ & + g_\sigma g_\rho^2\sigma\vec{\rho}_\mu\vec{\rho}^\mu \left(\alpha_2 + \frac{1}{2}\alpha'_2g_\sigma\sigma \right), \end{aligned} \quad (1)$$

with $F_{\mu\nu} = \partial_\nu\omega_\mu - \partial_\mu\omega_\nu$ and $\vec{B}_{\mu\nu} = \partial_\nu\vec{\rho}_\mu - \partial_\mu\vec{\rho}_\nu$. The nucleon mass is M and the meson masses are m_σ, m_ω , and m_ρ .

*Present address: Departamento de Física, Instituto Tecnológico de Aeronáutica, CTA, São José dos Campos, 12228-900. SP, Brazil

TABLE I: Set of updated constraints (SET2a) used in Ref. [4]. For more details concerning each constraint see the reference.

Constraint	Quantity	Density Region	Range of constraint
SM1	K_0	at ρ_0	190 – 270 MeV
SM3a	$P(\rho)$	$2 < \frac{\rho}{\rho_0} < 5$	Band Region
SM4	$P(\rho)$	$1.2 < \frac{\rho}{\rho_0} < 2.2$	Band Region
PNM1	$\mathcal{E}_{\text{PNM}}/\rho$	$0.017 < \frac{\rho}{\rho_0} < 0.108$	Band Region
MIX1a	J	at ρ_0	25 – 35 MeV
MIX2a	L_0	at ρ_0	25 – 115 MeV
MIX4	$\frac{S(\rho_0/2)}{J}$	at ρ_0 and $\rho_0/2$	0.57 – 0.86

We can derive from Eq.(1) the equation of state for symmetric nuclear matter ($\gamma = 4$). The pressure is given by

$$\begin{aligned}
P_{\text{NL}} = & -\frac{1}{2}m_\sigma^2\sigma^2 - \frac{A}{3}\sigma^3 - \frac{B}{4}\sigma^4 + \frac{1}{2}m_\omega^2\omega_0^2 + \frac{C}{4}(g_\omega^2\omega_0^2)^2 \\
& + g_\sigma g_\omega^2 \sigma \omega_0^2 \left(\alpha_1 + \frac{1}{2}\alpha'_1 g_\sigma \sigma \right) \\
& + \frac{\gamma}{6\pi^2} \int_0^\infty \frac{dk k^4}{(k^2 + M^{*2})^{1/2}} [n(k, T, \mu^*) + \bar{n}(k, T, \mu^*)],
\end{aligned} \tag{2}$$

where

$$\begin{aligned}
n(k, T, \mu^*) &= \frac{1}{e^{(E^* - \mu^*)/T} + 1}, \quad \text{and} \\
\bar{n}(k, T, \mu^*) &= \frac{1}{e^{(E^* + \mu^*)/T} + 1}
\end{aligned} \tag{3}$$

are the Fermi-Dirac distributions for particles and antiparticles, respectively. The effective energy, nucleon mass, and chemical potential are $E^* = (k^2 + M^{*2})^{1/2}$, $M^* = M - g_\sigma \sigma$, and $\mu^* = \mu - g_\omega \omega_0$, respectively. Furthermore, the (classical) mean-field values of σ and ω_0 are found by solving the following system of equations,

$$\begin{aligned}
m_\sigma^2 \sigma &= g_\sigma \rho_s - A\sigma^2 - B\sigma^3 + g_\sigma g_\omega^2 \omega_0^2 (\alpha_1 + \alpha'_1 g_\sigma \sigma) \\
m_\omega^2 \omega_0 &= g_\omega \rho - C g_\omega (g_\omega \omega_0)^3 - g_\sigma g_\omega^2 \sigma \omega_0 (2\alpha_1 + \alpha'_1 g_\sigma \sigma),
\end{aligned} \tag{5}$$

with

$$\rho = \frac{\gamma}{2\pi^2} \int_0^\infty dk k^2 [n(k, T, \mu^*) - \bar{n}(k, T, \mu^*)], \tag{6}$$

$$\rho_s = \frac{\gamma}{2\pi^2} \int_0^\infty \frac{dk M^* k^2}{(k^2 + M^{*2})^{1/2}} [n(k, T, \mu^*) + \bar{n}(k, T, \mu^*)]. \tag{7}$$

B. Density-dependent models

The four remaining parametrizations belong to the density-dependent group. Two of them include the δ

meson. Their Lagrangian density is given by

$$\begin{aligned}
\mathcal{L}_{\text{DD}} = & \bar{\psi}(i\gamma^\mu \partial_\mu - M)\psi + \Gamma_\sigma(\rho)\sigma\bar{\psi}\psi - \Gamma_\omega(\rho)\bar{\psi}\gamma^\mu\omega_\mu\psi \\
& - \frac{\Gamma_\rho(\rho)}{2}\bar{\psi}\gamma^\mu\vec{\rho}_\mu\vec{\tau}\psi + \Gamma_\delta(\rho)\bar{\psi}\vec{\delta}\vec{\tau}\psi - \frac{1}{4}F^{\mu\nu}F_{\mu\nu} \\
& + \frac{1}{2}(\partial^\mu\sigma\partial_\mu\sigma - m_\sigma^2\sigma^2) + \frac{1}{2}m_\omega^2\omega_\mu\omega^\mu - \frac{1}{4}\vec{B}^{\mu\nu}\vec{B}_{\mu\nu} \\
& + \frac{1}{2}m_\rho^2\vec{\rho}_\mu\vec{\rho}^\mu + \frac{1}{2}(\partial^\mu\vec{\delta}\partial_\mu\vec{\delta} - m_\delta^2\vec{\delta}^2),
\end{aligned} \tag{8}$$

where

$$\Gamma_i(\rho) = \Gamma_i(\rho_0)f_i(x); \quad f_i(x) = a_i \frac{1 + b_i(x + d_i)^2}{1 + c_i(x + d_i)^2}, \tag{9}$$

for $i = \sigma, \omega$, and $x = \rho/\rho_0$.

The expression for the pressure for these models can be obtained from Eq. (8) and reads:

$$\begin{aligned}
P_{\text{DD}} = & \rho\Sigma_R(\rho) - \frac{1}{2}m_\sigma^2\sigma^2 + \frac{1}{2}m_\omega^2\omega_0^2 \\
& + \frac{\gamma}{6\pi^2} \int_0^\infty \frac{dk k^4}{(k^2 + M^{*2})^{1/2}} [n(k, T, \mu^*) + \bar{n}(k, T, \mu^*)],
\end{aligned} \tag{10}$$

with the rearrangement term defined as

$$\Sigma_R(\rho) = \frac{\partial\Gamma_\omega}{\partial\rho}\omega_0\rho - \frac{\partial\Gamma_\sigma}{\partial\rho}\sigma\rho_s. \tag{11}$$

The mean-fields σ and ω_0 are given by

$$\sigma = \frac{\Gamma_\sigma(\rho)}{m_\sigma^2}\rho_s, \quad \text{and} \quad \omega_0 = \frac{\Gamma_\omega(\rho)}{m_\omega^2}\rho, \tag{12}$$

with the functional forms of ρ and ρ_s given as in the non-linear model, Eqs. (6)-(7), with the same distributions functions of Eq. (3), and the same form for the effective energy E^* . The effective nucleon mass and chemical potential are now given, respectively, by $M^* = M - \Gamma_\sigma(\rho)\sigma$, and $\mu^* = \mu - \Gamma_\omega(\rho)\omega_0 - \Sigma_R(\rho)$.

III. RESULTS

The necessary conditions used in the calculation of the critical point are given by the following expressions:

$$P_c = P(\rho_c, T_c), \quad \left. \frac{\partial P}{\partial\rho} \right|_{\rho_c, T_c} = 0, \quad \left. \frac{\partial^2 P}{\partial\rho^2} \right|_{\rho_c, T_c} = 0, \tag{13}$$

where P_c , ρ_c and T_c are, respectively, the critical pressure, density and temperature.

The critical parameters P_c , ρ_c , and T_c are then obtained for each of the CRMF parametrizations. The results can be seen in Table II.

The results we have computed can be compared with the ones obtained from eight experimental data Refs. [18–24]. In Table III we show a brief compilation of these results. In [24], the authors estimate not only the value

TABLE II: Critical values for Consistent RMF models

Model	Ref.	T_c (MeV)	ρ_c (fm $^{-3}$)	P_c (MeV/fm 3)
BKA20	[7]	14.92	0.0458	0.209
BKA22	[7]	13.91	0.0442	0.178
BKA24	[7]	13.83	0.0450	0.177
BSR8	[8]	14.17	0.0440	0.185
BSR9	[8]	14.11	0.0450	0.185
BSR10	[8]	13.90	0.0439	0.176
BSR11	[8]	14.00	0.0442	0.179
BSR12	[8]	14.15	0.0448	0.185
BSR15	[8]	14.53	0.0456	0.199
BSR16	[8]	14.44	0.0454	0.196
BSR17	[8]	14.32	0.0451	0.191
BSR18	[8]	14.25	0.0451	0.189
BSR19	[8]	14.28	0.0451	0.190
BSR20	[8]	14.41	0.0464	0.197
FSU-III	[9]	14.75	0.0461	0.205
FSU-IV	[9]	14.75	0.0461	0.205
FSUGold	[10]	14.75	0.0461	0.205
FSUGold4	[11]	14.80	0.0456	0.204
FSUGZ03	[12]	14.11	0.0450	0.185
FSUGZ06	[12]	14.44	0.0454	0.196
IU-FSU	[14]	14.49	0.0457	0.196
G2*	[13]	14.38	0.0468	0.192
Z271s2	[14]	17.97	0.0509	0.303
Z271s3	[14]	17.97	0.0509	0.303
Z271s4	[14]	17.97	0.0509	0.303
Z271s5	[14]	17.97	0.0509	0.303
Z271s6	[14]	17.97	0.0509	0.303
Z271v4	[14]	17.97	0.0509	0.303
Z271v5	[14]	17.97	0.0509	0.303
Z271v6	[14]	17.97	0.0509	0.303
DD-F	[15]	15.24	0.0505	0.245
TW99	[6]	15.17	0.0509	0.241
DDH δ	[16]	15.17	0.0509	0.241
DD-ME δ	[17]	15.32	0.0491	0.235

for $T_c = 17.9 \pm 0.4$ MeV, but also for $P_c = 0.31 \pm 0.07$ MeV/fm 3 , and $\rho_c = 0.06 \pm 0.01$ fm $^{-3}$, all of them related to symmetric nuclear matter.

By first analyzing the critical temperature, we can see that only the family Z271 (that encompasses all 8 related parametrizations), presents T_c compatible with five of the eight experimental points, including the more recent one [24]. The density-dependent models present the critical temperature inside the range of $15 \leq T_c \leq 19$ MeV proposed by [21]. The other critical parameters of Ref. [24], namely, pressure and density, are also compatible with the ones computed for the Z271 family. The density dependent family also agrees with this experiment.

TABLE III: Summary of experimental data of Refs. [18–24]

Reference	T_c (MeV)	ρ_c (fm $^{-3}$)	P_c (MeV/fm 3)
[18]	19 ± 3	-	-
[19]	16.60 ± 0.89	-	-
[20]	20 ± 3	-	-
[21]	17 ± 2	-	-
[22]	≥ 18	-	-
[23]	$19.5 \pm 1.2/16.5 \pm 1.0$	-	-
[24]	17.9 ± 0.4	0.06 ± 0.01	0.31 ± 0.07

If we look at the structure of Eq. (2), we can understand this agreement with the experimental data based on the only term that distinguish such model from the $\sigma^3 - \sigma^4$ one, which is those containing the C constant. In this case $C \neq 0$.

In the case of the density-dependent model, we can

think of a similar structure, since the nonlinear behavior of the σ field can be represented somehow in the thermodynamical quantities, by the density-dependent constant $\Gamma_\sigma(\rho)$. The same occurs with the ω_0 field, i.e., the strength of the repulsive interaction is also a density-dependent quantity, $\Gamma_\omega(\rho)$.

We have also tried to verify if there are correlations between the critical parameters and the observables of nuclear matter at zero temperature and at the saturation density. We investigate possible correlations between T_c , P_c and ρ_c with the symmetry energy, its slope and incompressibility. The results are shown in Figs. 1, 2, and 3, respectively.

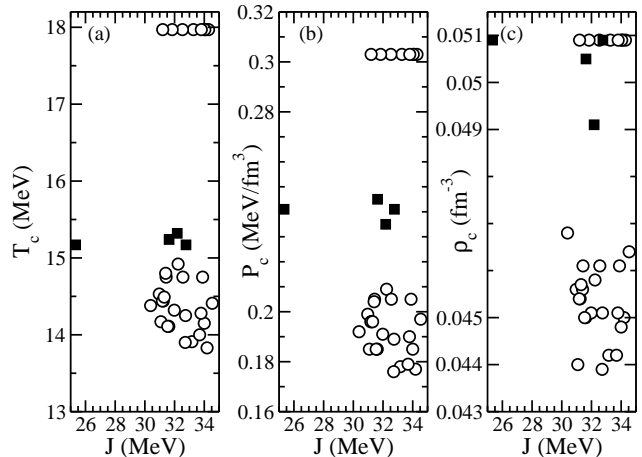


FIG. 1: Critical (a) temperature, (b) pressure, and (c) density of CRMF parametrizations versus symmetry energy at saturation density. Circles: nonlinear model. Squares: density dependent model.

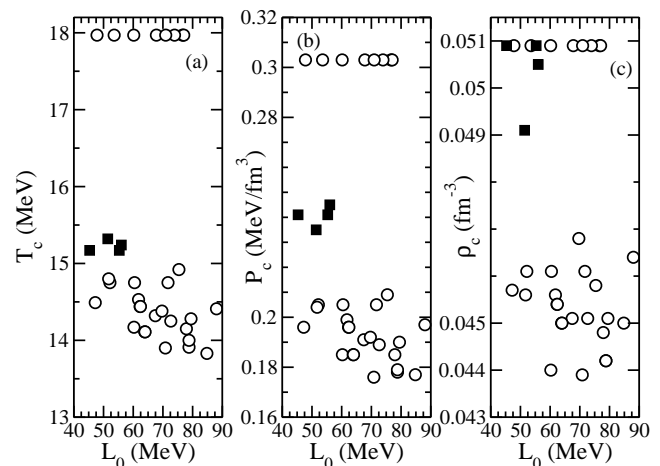


FIG. 2: Critical (a) temperature, (b) pressure, and (c) density of CRMF parametrizations versus the slope of symmetry energy at saturation density. Circles: nonlinear model. Squares: density dependent model.

Note that for the symmetry energy and its slope, Figs. 1 and 2, there are no indications of possible correlations. A unique pattern for the nonlinear and density-

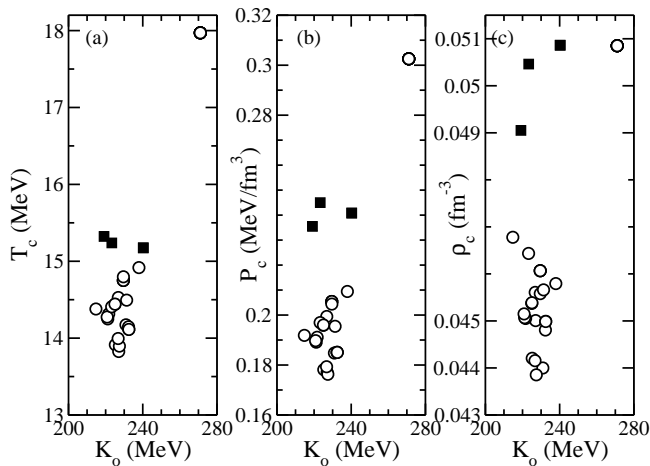


FIG. 3: Critical (a) temperature, (b) pressure, and (c) density of CRMF parametrizations versus incompressibility at saturation density. Circles: nonlinear model. Squares: density dependent model.

dependent models are not seen. However, the picture changes when we look at the incompressibility (K_0). From Fig. 3, one can observe an increasing behavior of T_c , P_c and ρ_c as K_0 increases.

IV. SUMMARY

In this work, we present the results obtained in the calculation of the critical parameters: temperature, pres-

sure, and density in symmetric nuclear matter. In our analysis, we verified that the nonlinear models, whose parameterizations were grouped in the family Z271, show a good agreement with the experimental data [24] for all critical parameters analyzed. The density-dependent family also shows an agreement with the data given in [24] for the pressure and density. Concerning T_c , the agreement is only found with data presented in Ref. [21].

In the search for possible correlations, we can see that the incompressibility at zero temperature and at saturation density show a clear increasing behavior with the critical parameters analyzed. The same does not occur with the symmetry energy and its slope.

Acknowledgments

This work was partially supported by Conselho Nacional de Desenvolvimento Científico e Tecnológico (CNPq), Brazil under grants 301155/2017-8 and 310242/2017-7. This work is also a part of the project CNPq-INCT-FNA Proc. No. 464898/2014-5.

-
- [1] O. Lourenço, M. Dutra, and D. P. Menezes, *Phys. Rev. C* **95**, 065212 (2017)
 - [2] J. B. Silva, O. Lourenço, A. Delfino, J. S. Sá Martins, M. Dutra, *Phys. Lett. B* **664** 246, (2008).
 - [3] S.S. Avancini, L. Brito, Ph. Chomaz, D.P. Menezes and C. Providência, *Phys. Rev. C* **74**, 024317 (2006).
 - [4] M. Dutra, O. Lourenço, S. S. Avancini, B. V. Carlson, A. Delfino, D. P. Menezes, C. Providência, S. Typel, and J. R. Stone, *Phys. Rev. C* **90**, 055203 (2014).
 - [5] M. Dutra, O. Lourenço, and D. P. Menezes, *Phys. Rev. C* **93**, 025806 (2016); Erratum: *Phys. Rev. C* **94**, 049901(E) (2016).
 - [6] S. Typel and H. H. Wolter. *Nucl. Phys. A* **656**, 331 (1999).
 - [7] B. K. Agrawal. *Phys. Rev. C* **81**, 034323 (2010).
 - [8] S. K. Dhiman. R. Kumar. and B. K. Agrawal. *Phys. Rev. C* **76**, 045801 (2007).
 - [9] B.-J. Cai. L.-W. Chen. *Phys. Rev. C* **85**, 024302 (2012).
 - [10] B. G. Todd-Rutel and J. Piekarewicz. *Phys. Rev. Lett.* **95**, 122501 (2005).
 - [11] J. Piekarewicz and S. P. Weppner. *Nucl. Phys. A* **778**, 10 (2006).
 - [12] R. Kumar. B. K. Agrawal. and S. K. Dhiman. *Phys. Rev. C* **74**, 034323 (2006).
 - [13] A. Sulaksono and T. Mart. *Phys. Rev. C* **74**, 045806 (2006).
 - [14] F. J. Fattoyev. C. J. Horowitz. J. Piekarewicz. and G. Shen. *Phys. Rev. C* **82**, 055803 (2010).
 - [15] T. Klähn. *et al.*. *Phys. Rev. C* **74**, 035802 (2006).
 - [16] T. Gaitanos. M. Di Toro. S. Typel. V. Baran. C. Fuchs. V. Greco. and H. H. Wolter. *Nucl. Phys. A* **732**, 24 (2004).
 - [17] X. Roca-Maza. X. Viñas. M. Centelles. P. Ring. and P. Schuck *Phys. Rev. C* **84**, 054309 (2011).
 - [18] V. A. Karnaukhov, *Phys. At. Nucl.* **60**, 1625 (1997).
 - [19] J. B. Natowitz, K. Hagel, Y. Ma, M. Murray, L. Qin, R. Wada, and J. Wang, *Phys. Rev. Lett.* **89**, 212701 (2002).
 - [20] V. A. Karnaukhov, et al., *Phys. Rev. C* **67**, 011601(R) (2003).
 - [21] V. A. Karnaukhov et al., *Nucl. Phys. A* **734**, 520 (2004).
 - [22] V. A. Karnaukhov et al., *Nucl. Phys. A* **780**, 91 (2006).
 - [23] V. A. Karnaukhov, *Phys. At. Nucl.* **71**, 2067 (2008).
 - [24] J. B. Elliott, P. T. Lake, L. G. Moretto, and L. Phair, *Phys. Rev. C* **87**, 054622 (2013).